Buckling and Postbuckling of Delaminated Composites Under Compressive Loads Including Transverse Shear Effects

G. A. Kardomateas* and D. W. Schmueser†
General Motors Research Laboratories, Warren, Michigan

The deformation of delaminated composites under axial compression is analyzed by a one-dimensional beam-plate model. In this model, a formulation that accounts for the transverse shear effects is also presented. With the perturbation technique, analytical solutions for the critical instability load and the postbuckling deflections are obtained. All possible instability modes, namely, local delamination buckling, global plate buckling, and coupled global and local (mixed) buckling, are considered. Specific emphasis is placed on studying the transverse shear effects on both the critical load and the postcritical characteristics, as well as the influence of the geometry such as that of the location of the delamination across the thickness. The postbuckling solution is used in conjunction with a *J*-integral formulation to study the postcritical characteristics with respect to possible quasistatic extension of the delamination and the energy absorption capacity of a beam.

Nomenclature

A_i	= cross-sectional areas
D_i	= bending stiffnesses
D_{12}	= shear modulus
E_1	= Young's modulus in the axial direction
G	= energy-release rate
H	= thickness of the delamination
k_i	$=\sqrt{P_{i,0}/D_i}$
L	= length of the beam/plate
ℓ	= delamination length
M_i	= bending moments
P_i	= axial forces
T	= thickness of the beam/plate
α	= section parameter
ν_{13}, ν_{31}	= Poisson's ratio
ϕ	= angle at the section where the delamination starts
Subscripts	
b	= base plate
l	= lower part
u	= upper part
1	= in-plane longitudinal direction
2	= normal (out-of-plane) direction
3	= in-plane transverse direction

Introduction

DELAMINATION (separation of adjoining plies) has been a subject of concern in engineering applications of composite materials because of the resulting reduction in load-bearing capacity and degradation of structural integrity and stiffness. Delaminations may be developed during the production phase because of manufacturing imperfections or during the operational phase due to, for example, impact of foreign objects. Under compression loading, the delaminated layer may buckle, and interlaminar separation from growth of the delamination may follow.

Delamination buckling may, however, be a desirable damage mechanism from an energy absorption viewpoint, because of the large displacements involved in the postbuckling stages, as opposed to the small strains that characterize fiber and matrix fracture. Recent experimental studies that we performed in order to characterize the bending performance of composite test specimens have shown that delamination (separation of adjoining plies) is the primary failure mechanism for the compressively loaded beam face. As illustrated in Fig. 1, taken from a static crush test on a Kevlar/epoxy beam, delamination of composite laminae exhibit failure zones that can be considered as the corollary of the plastic hinge formation that governs bending-induced failure of metallic beams.

Hence, there is a need for understanding the mechanics of delamination failure that would enable the proper designing of composite parts. The problem has been dealt with by several investigators.[1-6] Furthermore, it has been shown[3-5] that the stability problem may involve local buckling of the delamination or combined local and global buckling (buckling of both the delamination layer and the overall plate). Our work differs from the other investigations in a number of ways, and, as will be evident in what follows, the approach based on the perturbation technique that we use leads to explicit analytical expressions for the initial postbuckling behavior.

In studying buckling instability in composites, consideration should be given to the effect of the transverse shearing force that is introduced by the deflection. Consider an orthotropic homogeneous linearly elastic material with the x, y, z or 1, 2, 3 notation referring to the in-plane longitudinal, normal (out-of-plane), and in-plane transverse direction. It is known[7] that inclusion of transverse shear effects reduces the critical buckling load for a beam column of length ℓ, cross-sectional area A, and moment of inertia I by approximately the factor $1/(1+\alpha\pi^2 E_1 I/4\ell^2 A G_{12})$, where α is a numerical factor depending on the shape of the cross section ($\alpha = 1.2$ for a rectangular cross section) and E and G are the extensional and shear moduli. For example, in a unidirectional laminate, where the principal material direction ℓ coincides with the axis of the beam column, the ratio $E_\ell/G_{\ell t}$ is much greater for composite laminates that for their metal counterparts.[8] Thus, although the factor just given is very nearly equal to unity for metals, it can be significantly larger for composite materials, making predictions based on neglecting this effect nonconservative. A formulation that accounts for the effects of transverse shear will be presented in this work.

To solve the stability problem, the perturbation or small parameter method[9] is used in this work. The method consists, in general, of developing the solution in powers of a parameter that either appears explicitly in the problem or is introduced

Received Jan. 26, 1987; presented as Paper 87-0877 at the AIAA 28th Structures, Structural Dynamics and Materials Conference, Monterey, CA, April 6-8, 1987; revision received Aug. 10, 1987.

*Senior Research Engineer, Engineering Mechanics Department.
†Staff Research Engineer, Engineering Mechanics Department.

artificially. The perturbation is generated in the neighborhood of the solution for the initial (before instability) system such that the known properties of the initial system can be utilized for the solution to the perturbed system. An analytical solution for the postbuckling deflections of the delaminated composite will thus be presented.

In general, a Griffith-type fracture criterion has been used to study delamination growth. The energy-release rate has been computed either by a numerical differentiation of the total potential energy[2] with respect to the delamination length or by evaluating the path-independent J-integral.[10] The latter method allows a straightforward evaluation of the energy-release rate in terms of the axial forces and bending moments acting across the various cross sections adjacent to the tip of the delamination. This method will be used here after being modified to include transverse shear effects.

Analysis

Instability modes and Governing Equations

In the present analysis, the configuration under study is represented in the sketch of Fig. 2 and consists of a homogeneous, orthotropic beam plate of thickness T and of unit width containing a single delamination at depth $H(H \leq T/2)$ from the top surface of the plate. The plate is assumed to be clamped-clamped and subjected to an axial compressive force P at the ends. The delamination is symmetrically located in the center of the beam. Over this region, the laminate consists of the part above the delamination, of thickness H referred to as the "upper" part, and the part below the delamination, of thickness $T-H$ referred to as the "lower" part. The section near each end where the laminate is intact and of thickness T is referred to as the "base" laminate. The coordinate systems for the separate parts are shown in Fig. 3.

The laminate is loaded, and at the critical level three different possible modes of instability can be identified. First, global buckling of the whole beam may occur before any other deflection pattern takes place. Second, both local and global buckling, involving transverse deflections for both the upper and lower parts as well as the base plate, may occur and we will call this "mixed" buckling. Third, only local buckling of the delaminated upper layer may occur, the lower part and the base plate remaining flat. The latter instability mode has been also referred to as "thin film delamination."[2]

Let us develop the governing equations for the general mixed buckling case. The differential equations for the deflections of the different parts (upper delaminated layer, lower part, and base plate) can be written[7]

$$D_i \frac{d^4 Y_i}{dx^4} + P_i \frac{d^2 y_i}{dx^2} = 0 \tag{1}$$

In Eq. (1), D_i is the bending stiffness, $D_i = E_1 t_i^3/[12(1-\nu_{13}\nu_{31})]$, t_i being the thickness of the corresponding part. The coordinate systems have been selected to satisfy the boundary conditions

$$\begin{aligned} y_i &= 0 \quad \text{at} \quad x = 0, \ell \quad \text{for} \quad i = u, l \\ y_i &= 0 \quad \text{at} \quad x = 0 \quad\quad \text{for} \quad i = b \end{aligned} \tag{2}$$

These different parts have a common section where the delamination starts. The corresponding force and moments at this interface for the different parts are denoted by P_i, M_i (Fig. 3). Force and moment equilibrium at this section give

$$P_u + P_l = P_b = P \tag{3}$$

$$M_u + M_l + P_u\left(\frac{T-H}{2}\right) - P_l\left(\frac{H}{2}\right) = M_b \tag{4}$$

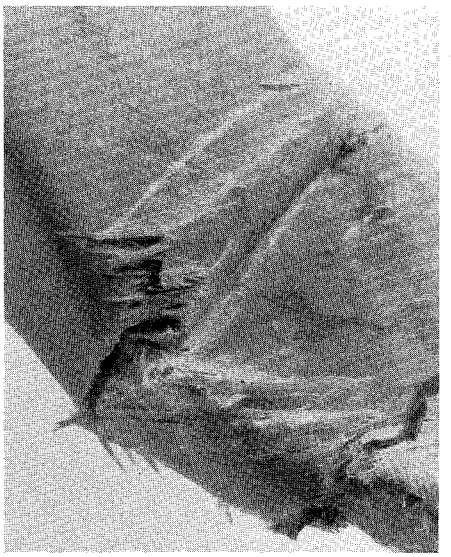

Fig. 1 Delamination buckling on the compressive face of a statically crushed composite beam.

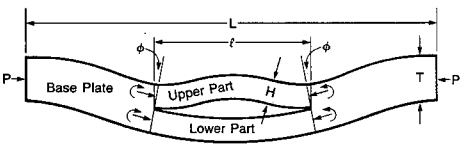

Fig. 2 Delamination/buckling geometry

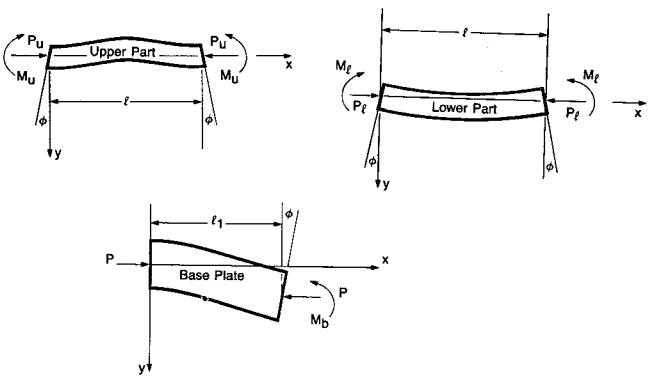

Fig. 3 Definition of the coordinate systems.

The deflections of the upper and lower parts should be geometrically compatible. Thus, a second condition necessary for a solution involves the compatible shortening of the upper and lower parts, which is expressed as

$$(1-\nu_{13}\nu_{31})\frac{P_u \ell}{A_u E_1} - (1-\nu_{13}\nu_{31})\frac{P_l \ell}{A_l E_1} + \frac{1}{2}\int_0^\ell y_u'^2 dx - \frac{1}{2}\int_0^\ell y_l'^2 \, dx = T y_u' x = 0 \tag{5}$$

In Eq. (5), A_u, A_l are the cross-sectional areas of the upper and lower part. Notice that at the common section

$$y_u'|_{x=0} = y_l'|_{x=0} = y_b'|_{x=\ell} \tag{6}$$

An obvious solution of Eqs. (3–5) is $P_u = PH/T$, $P_l = P(T-H)/T$, $y_u(x) = y_l(x) = y_b(x) = 0$. This is the state of stress befor instability, with no transverse deflections.

Two limiting instability modes can be readily identified (Fig. 4). First, the load required for global buckling, that is, the buckling load of the composite beam plate as a whole including transverse shear, is slightly smaller than the Euler load P_{eul} and is given by[7]

$$P_{\text{glo}} = \frac{\sqrt{1 + 4\alpha P_{\text{eul}}/(A_b G_{12})} - 1}{2\alpha/(A_b G_{12})}; \quad P_{\text{eul}} = \frac{4\pi^2 E_1 T^3}{12(1 - \nu_{13}\nu_{31})L^2} \tag{7}$$

This case of global buckling preceding any other instability mode would occur for a relatively small delamination length.

On the other hand, if the length of the delamination is ralatively large, then local buckling of the delaminated layer precedes any other mode of instability because the delamination is sufficiently slender in comparison with the whole plate. In this case, the only out-of-plane displacement is that of the upper detached segment. The critical compressive force at the upper segment including transverse shear effects $P_{u,\text{cr}}$ is again slightly smaller than the Euler load $P_{u,\text{eul}}$ and is given by[7]

$$P_{u,\text{cr}} = \frac{\sqrt{1 + 4\alpha P_{u,\text{eul}}/(A_u G_{12})} - 1}{2\alpha/(A_u G_{12})} \tag{8a}$$

$$P_{u,\text{eul}} = \frac{4\pi^2 E_1 H^3}{12(1 - \nu_{12}\nu_{31})\ell^2} \tag{8b}$$

Thus, an upper limit on the applied load P, corresponding to the instability being initiated by the local buckling of the upper part, is taken to be

$$P_{\text{loc}} = (T/H)P_{u,\text{cr}} \tag{9}$$

If the critical instability load is smaller than P_{glo} and P_{loc}, then combined local and global buckling involving out-of-plane deflections for both the delaminated layer and the base plate takes place. This general case is dealt with in detail in the next section.

Buckling

The perturbation procedure used here to solve Eq. (1) in conjunction with the boundary conditions (2) and (6) is briefly outlined. Initially, as the compressive load P is being applied, the plate remains flat at a state of pure compression and the solution for the upper delaminated part u, lower part l, and base plate outside the delaminated region (b) is

$$\begin{aligned} &y_{u,0}=0, \quad M_{u,0}=0, \quad P_{u,0}=P_0H/T \\ &y_{l,0}=0, \quad M_{l,0}=0, \quad P_{l,0}=P_0(T-H)/T \\ &y_{b,0}=0, \quad M_{b,0}=0, \quad P_{b,0}=P_0 \end{aligned} \tag{10}$$

Let the angle at the interface of the delaminated and base plate be denoted by ϕ. The deflection and load quantities at each part, $y_i(x)$, P_i, M_i, are developed into ascending perturbation series with respect to ϕ.

$$\begin{aligned} y_i(x) &= \phi y_{i,1}(x) + \phi^2 y_{i,2}(x) + \cdots \\ P_i &= P_{i,0} + \phi P_{i,1} + \phi^2 P_{i,2} + \cdots \\ M_i &= \phi M_{i,1} + \phi^2 M_{i,2} + \cdots \end{aligned} \tag{11}$$

By definition, at this interface, defined by $x = 0$ for $i = u,l$ and by $x = \ell_1 = (L - \ell)/2$ for $i = b$ (Fig. 3)

$$y_{i,1}{}' = 1, \quad y'_{i,2} = y'_{i,3} = \cdots = 0 \tag{12}$$

at the common section.

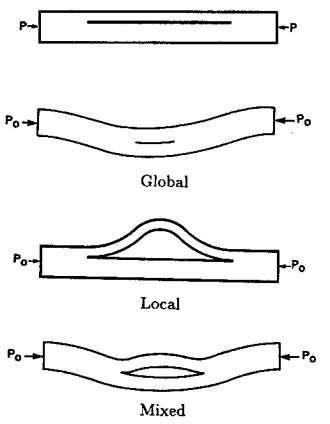

Fig. 4 Instability modes for a delaminated composite.

Substituting Eq. (11) into the differential equation (1) and equating like powers of ϕ lead to a series of linear differential equations and boundary conditions for each part. In the first approximation, the terms in the first power of ϕ are equated and we obtain the small deflection equation

$$D_i y_{i,1}^{(4)} + P_{i,0} y''_{i,1} = 0$$

The solution for the upper and lower parts should fulfill the requirements of symmetry; for example, $y'_{,1}(0) = -y'_{i,1}(\ell)$, and the boundary conditions

$$y_{i,1} = 0 \quad \text{at} \quad x = 0, \ell \quad \text{for} \quad i = u, l$$

The base plate should fulfill the conditions of the end fixity. For a delaminated clamped-clamped plate, these are

$$y_{b,1} = 0, \quad y'_{b,1} = 0 \quad \text{at} \quad x = 0$$

The solution, satisfying Eq. (12), is given for $i = u,l$ by

$$y_{i,1} = \frac{1}{k_{i,0}\sin(k_{i,0}\ell/2)}\left[\cos\left(\frac{k_{i,0}\ell}{2} - k_{i,0}x\right) - \cos\frac{k_{i,0}\ell}{2}\right] \tag{13}$$

$$k_{i,0}^2 = P_{i,0}/D_i$$

and for the base plate outside the delamination,

$$y_{b,1} = \frac{(1 - \cos k_{b,0}x)}{k_{b,0}\sin k_{b,0}\ell_1} \tag{14}$$

$$k_{b,0}^2 = P_0/D_b, \qquad \ell_1 = (L - \ell)/2$$

The associated equilibrium and compatibility equations (3-5) up to the order ϕ are given in terms of the moments at the interface

$$M_{u,1} + M_{l,1} - M_{b,1} = P_{l,1}H/2 - P_{u,1}(T - H)/2 \tag{15}$$

and

$$T\frac{EH(T-H)}{2\ell(1-\nu_{123}\nu_{31})} = P_{u,1}(T-H)/2 - P_{l,2}H/2 \tag{16}$$

The end moments $M_{i,1} = -D_i y''_i$ are given from Eqs. (13) and (14) in terms of the first-order quantities. Substituting those expressions into the aforementioned two equations and elim-

inating the quantity $P_{l,1}H/2-P_{u,1}(T-H)/2$ give an equation for the critical buckling load P_0 as follows:

$$H^3k_{u,0}\cot(k_{u,0}\ell/2)+(T-H)^3k_{l,0}\cot(k_{l,0}\ell/2)$$
$$+T^3k_{b,0}\cot k_{b,0}\ell_1+6TH(T-H)/\ell=0 \tag{17}$$

Postbuckling

When the terms in ϕ^2 are equated, the following differential equations are obtained from Eq. (1):

$$D_iy_{i,2}^{(4)}+P_{i,0}y_{i,2}''=-P_{i,1}y_{i,1}''$$

The second-order solution for the upper and lower parts should again fulfill the requirements of symmetry and the boundary conditions

$$y_{i,2}=0 \quad \text{at} \quad x=0,\ell \quad \text{for} \quad i=u,\ell$$

For the base plate, it should fulfill the conditions of the end fixity.

$$y_{b,2}=0 \quad y_{b,2}'=0 \quad \text{at} \quad x=0$$

The solution to the second-order problem is a superposition of the general solution and a particular solution. For the upper and lower parts, it is given as

$$y_{i,2}=c_{i2}\left[\cos\left(\frac{k_{i,0}\ell}{2}-k_i,0^\alpha\right)-\cos\frac{k_i,0^\ell}{2}\right]$$
$$+\frac{P_{i,1}}{2D_ik_{i,0}^2\sin(k_{i,0}\ell/2)}\left[\left(x-\frac{\ell}{2}\right)\sin\left(\frac{k_{i,0}\ell}{2}-k_i,0^\alpha\right)+\frac{\ell}{2}\sin\frac{k_{i,0}\ell}{2}\right] \tag{18}$$

The constant c_{i2} is found from Eq. (12) in terms of $P_{i,1}$

$$c_{i2}=-\frac{P_{i,1}}{2D_ik_{i,0}^3\sin^2(k_{i,0}\ell/2)}\left(\sin\frac{k_{i,0}\ell}{2}+\frac{\ell k_i,0}{2}\cos\frac{k_{i,0}\ell}{2}\right)$$

For the base plate, we find similarly the second-order solution by

$$y_{b,2}=c_{b,2}(1-\cos k_{b,0}x)+\frac{P_{b,1}}{2D_bk_{b,0}^2\sin k_{b,0}\ell_1}x\sin k_{b,0}x \tag{19}$$

and, from Eq. (12),

$$c_{b,2}=\frac{P_{b,1}}{2D_bk_{b,0}^3\sin^2(k_{b,0}\ell_1)}(\sin k_{b,0}\ell_1+\ell_1k_{b,0}\cos k_{b,0}\ell_1)$$

The equilibrium equation (4) for the second-order terms is, in turn,

$$M_{u,2}+M_{l,2}-M_{e,2}=P_{l,2}H/2-P_{u,2}(T-H)/2 \tag{20}$$

The geometric compatibility equation (5) for the second-order terms is expressed as

$$\frac{1}{2}\int_0^\ell y_{u,1}'^2\,dx-\frac{1}{2}\int_0^\ell y_{l,1}'^2\,dx=\frac{2(1-\nu_{13}\nu_{31})\ell}{E_1H(T-H)}$$
$$\times\left[P_{l,2}H/2-P_{u,2}(T-H)/2\right] \tag{21}$$

Notice that the second-order moments $M_{i,2}=-D_iy_{i,2}''$ at the interface are given from Eqs. (18) and (19) in terms of the (yet undetermined) first-order quantities. Thus, eliminating the quantity $P_{l,2}H/2-P_{u,2}(T-H)/2$ from Eqs. (20) and (21) gives the following equation for the first-order forces $P_{u,1}$ and $P_{l,1}$:

$$P_{u,1}\left[\frac{\cos k_{b,0}\ell_1}{2k_{b,0}\sin k_{b,0}\ell_1}-\frac{\ell_1\cos^2k_{b,0}\ell_1}{2\sin^2k_{b,0}\ell_1}-\frac{\ell_1}{2}-\frac{\ell\cos^2(k_{u,0}\ell/2)}{4\sin^2(k_{u,0}\ell/2)}\right.$$
$$\left.+\frac{\cos(k_{u,0}\ell/2)}{2k_{u,0}\sin(k_{u,0}\ell/2)}-\frac{\ell}{4}\right]$$
$$+P_{l,1}\left[\frac{\cos k_{b,0}\ell_1}{2k_{b,0}\sin k_{b,0}\ell_1}-\frac{\ell_1\cos^2k_{b,0}\ell_1}{2\sin^2k_{b,0}\ell_1}-\frac{\ell_1}{2}\right.$$
$$\left.-\frac{\ell\cos^2(k_{l,0}\ell/2)}{4\sin^2(k_{l,0}\ell/2)}+\frac{\cos(k_{l,0}\ell/2)}{2k_{l,0}\sin(k_{l,0}\ell/2)}-\frac{\ell}{4}\right]$$
$$=\left[\frac{\sin(k_{l,0}\ell)-k_{l,0}\ell}{k_{l,0}\sin^2(k_{l,0}\ell/2)}-\frac{\sin(k_{u,0}\ell)-k_{u,0}\ell}{k_{u,0}\sin^2(k_{u,0}\ell/2)}\right]\frac{E_1H(T-H)}{8\ell(1-\nu_{13}\nu_{31})} \tag{22}$$

The second equation needed for finding $P_{u,1}$, $P_{l,1}$ is the first-order equilibrium equation (15) at the interface, namely,

$$P_{l,1}H/2-P_{u,1}(T-H)/2=\frac{P_{u,0}}{k_{u,0}\tan(k_{u,0}\ell/2)}$$
$$+\frac{P_{l,0}}{k_{l,0}\tan(k_{l,0}\ell/2)}+\frac{P_0}{k_{b,0}\tan k_{b,0}\ell_1} \tag{23}$$

The foregoing system of linear equations allows finding $P_{u,1}$ and $P_{l,1}$ and hence the first-order applied force $P_1=P_{u,1}+P_{l,1}$. The solution for the third-order problem is given in the appendix.

Transverse Shear Effects

As was noted in the introduction, in studying stability problems of composite materials, consideration should be given to the effect of the transverse shearing force that is introduced by the deflection. This is due to the relatively low ratio of shear to extensional modulus of composites as opposed to their metal counterparts.

To correct for this effect, let us first consider the differential equations of the deflection curve. When buckling occurs, there will be a component $Q=P\sin\theta\simeq P\theta$ of the compressive axial force P acting on the cross sections (Fig. 5). Thus, in addition to the angle θ between the x axis direction and the normal to the cross section (change in slope due to the bending moment M), there is an additional slope, due to shearing strains, of $\alpha Q/AG_{12}$ (where α is a numerical factor depending on the shape of the cross section), measured from the normal to the tangent of the axis of the deflected beam.[6] Therefore, the slope of the deflected curve is

$$\frac{dy}{dx}=\theta+\frac{\alpha P\theta}{AG_{12}}$$

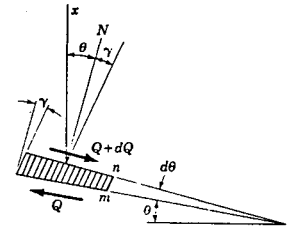

Fig. 5 Deformation due to the transverse shear component of the axial force.

Since $d\theta/dx = M/D$, we obtain the following expression for curvature:

$$\frac{d^2y}{dx^2} = \frac{M}{D}\left(1 + \frac{\alpha P}{AG_{12}}\right)$$

and the differential equation for the deflection,[7] modified to include transverse shear effects, may be written

$$\frac{D}{1 + \alpha P/AG_{12}} \frac{d^4y}{dx^4} + P\frac{d^2y}{dx^2} = 0 \tag{24}$$

Thus, we may account for the effect of transverse shear by replacing the rigidity D with the reduced rigidity $D^* = D/(1 + \alpha P_0/AG_{12})$ (where we have substituted the critical load P_0, since we are interested in the behavior around this point) that, in the foregoing solution, would mainly change the definition of k. For example,

$$k_{b,0}^2 = \frac{12(1 - \nu_{13}\nu_{31})P_0(1 + \alpha P_0/A_bG_{12})}{E_1T^3}$$

Discussion of Numerical Results

Numerical examples are presented for Kevlar/epoxy, graphite/epoxy, and glass/epoxy composites. The elastic constants typical of these materials are given in Table 1. In including transverse shear effects, a rectangular cross section ($\alpha = 1.2$) was assumed. In the examples, the filaments are parallel to the x axis. The different regions of buckling instability can be identified in the plots of the critical instability load, normalized with respect to the Euler load for the delaminated layer, $4\pi^2E_1H^3/12(1 - \nu_{13}\nu_{31})\ell^2$, vs delamination length (Fig. 6). The characteristic equation (17) is solved for the critical load P_{0c}. If $P_{0c} < (P_{glo}, P_{loc})$, as given by Eqs. (7) and (9), then combined mixed buckling involving out-of-plane deflections for both the delaminated layer and the base plate takes place. For short delamination lengths, global buckling is dominant, whereas for relatively large lengths, local buckling of the delaminated layer occurs first. In addition, the range of mixed (combined local and global) buckling is smaller if the delamination is located closer to the surface (larger T/H). In the case of $T/H = 24$, it is seen that the instability load can be determined essentially by the simple formulas (7) and (9). The effect of material parameters is illustrated in Fig. 7. It is seen that the range of the different instability modes is not affected by the material data, whereas the increased instability load of the higher modulus graphite/epoxy is expected.

Finally, the effect of transverse shear on the buckling load is shown in Fig. 8 for the case of graphite/epoxy with $T/H = 15$ and $L/H = 200$. Including these effects is expected to lower the value of the critical load. The decrease is larger in the midsection of the curve (mixed buckling). For this example, it is as much as 20% for $\ell/H = 30$ and only about 3% for $\ell/H = 100$. The extent of the regions of different instability modes is not, however, affected.

Growth Characteristics

As Fig. 1 shows, unlike metallic beams that absorbed energy via plastic hinge formation under bending loads, the composite beams exhibited delamination buckling on their compressive faces. The postcritical deformation, both before and after the growth of the delaminated regions, strongly affects the energy-absorption characteristics. Thus, the postbuckling solution that has been obtained in the previous section will be used in the following to investigate the postcritical characteristics.

The midpoint deflections of the upper and lower parts as given by the aforementioned postbuckling solution have been plotted in Fig. 9 as a function of the applied compressive load for the example case of $T/H = 6$, $L/H = 200$, and delamination length $\ell/H = 60$, which corresponds to mixed buckling. The fact worth mentioning is that the initial postbuckling geometry under increasing applied load is characterized by a negative angle at the interface ϕ that causes both the upper and lower parts to be deflected upward; the deflection of the lower part is two orders of magnitude smaller than that of the delaminated layer. This behavior was also predicted in Ref. 4 by an order-of-magnitude analysis.

The initiation and subsequent process of delamination growth can now be analyzed on the basis of a Griffith-type fracture criterion. Predicting whether the delamination will

Table 1 Material constants

Material	E_ℓ GN/m^2	E_t GN/m^2	G_{tt} GN/m^2	ν_{tt}
Graphite-epoxy	215	6.5	3.2	0.26
Kevlar-epoxy	70	4.5	2.5	0.35
Glass-epoxy	53	14	8.6	0.26

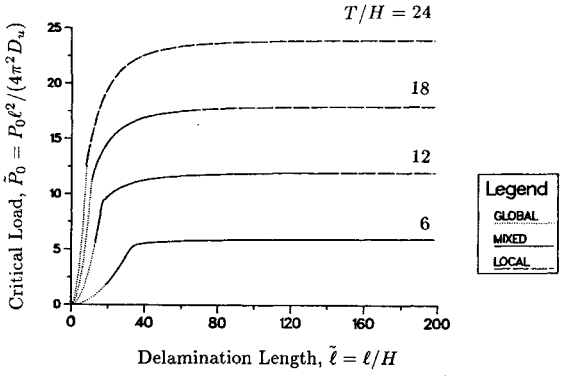

Fig. 6 Effect of delamination location on the buckling load (Kevlar/epoxy, $L/H = 200$, transverse shear effects included).

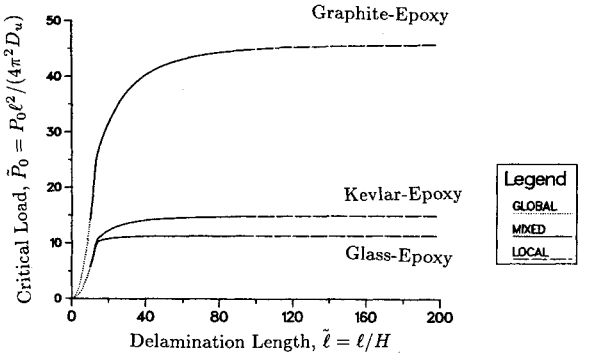

Fig. 7 Effect of material properties on the buckling load ($T/H = 15$, $L/H = 200$, transverse shear effects included). The modulus of the Kevlar/epoxy has been used in normalizing the load.

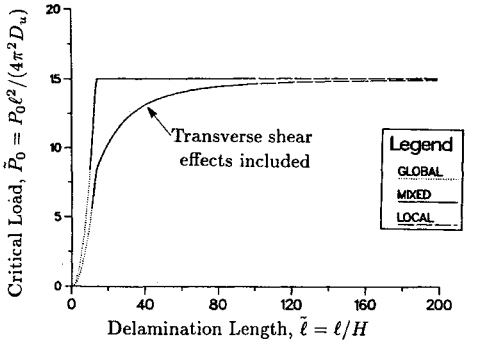

Fig. 8 Effect of transverse shear on the instability load for graphite/epoxy, $T/H = 15$, $L/H = 200$.

grow requires an evaluation of the energy-release rate. This quantity is the differential of the total potential energy with respect to the delamination length.[2] Alternatively, the path-independent J-integral concept[11] may be used to derive the energy-release rate from the current stress and displacement distribution. The latter method was applied for a one-dimensional delamination[10] and resulted in an algebraic expression for the energy-release rate in terms of the axial forces and bending moments acting across the various cross sections adjacent to the tip of the delamination. This expression can also be modified to account for the effect of transverse shear. The rate of change of slope produced by the shearing force Q represents the additional curvature due to shear. Following the same argument as in deriving the differential equation for the deflections in the previous section, we can include this additional term in the equation for the moments and, hence, modify accordingly the equation for the energy-release rate. In terms of the quantities

$$P^* = P(H/T) - P_u,\ M^* = M_u,\ M^{**} = P^*T/2 - M^*$$

the energy-release rate per unit width is expressed as

$$G = \frac{12(1-\nu_{13}\nu_{31})}{2E_1(T-H)}\left\{P^{*2} + 12(M^*/H)^2 [1-\alpha P^*/(A_uG)]^2\right\} + \frac{12(1-\nu_{13}\nu_{31})}{2E_1(T-H)} \times \left\{P^{*2} + 12[M^{**}/(T-H)]^2[1+\alpha P^*/(A_lG)]^2\right\} \quad (25)$$

The relation between the nondimensional strain energy-release rate, $\bar{G} = G/(ET^5/L^4)$, and applied load normalized so as to be independent of delamination length, $\bar{P} = P/[4\pi^2E_1T^3/12(1-\nu_{13}\nu_{31})L^2]$, is plotted in Fig. 10 for the example case of $T/H = 6$, $L/H = 200$ and two close values of the delamination length, $\ell/H = 60,61$ (buckling instability of the mixed type).

After initial buckling, whether further delamination occurs depends on the magnitude of the fracture energy G_c, defined as the energy required to produce a unit of new delamination. As Fig. 10 shows, the energy-release rate increases with increasing applied load during initial postbuckling. Furthermore, the force P corresponding to a constant G decreases with delamination growth. Hence, if G_c is relatively small, allowing growth to start, delamination growth under a constant applied load is generally a catastrophic process. For materials of greater G_c, the load may increase substantially beyond the buckling load before the energy-release rate reaches the critical value, at which point delamination growth starts and proceeds catastrophically unless the load decreases. It should be born in mind that in Fig. 10, $\bar{G}_c$ is the normalized energy-release rate, $\bar{G}_c = G_c/(ET^5/L^4)$ and, thus, although G_c is a material constant, $\bar{G}_c$ depends on the geometry being larger for a thinner plate.

The transverse shear effects are also illustrated in Fig. 10. Including these effects results in a steeper $G-P$ curve, which indicates that transverse shear effects would promote the onset of growth and that more energy (the energy of the transverse shear forces) would be released per unit applied load. Another effect worth considering is that of the lay-up angle. This is shown in Fig. 11, which gives the energy-release rate as a function of the applied load for three different lay-up angles (transverse shear effects were not included in this example). Scales of the same length for the applied load (corresponding to the different critical load in each case) have been used. The noteworthy feature is the increase in the slope of the $G-P$ curves with the higher lay-up angles. This means that growth could occur earlier and that there will be potentially more energy absorbed since the energy released per unit applied load is higher. Indeed, static bend tests of Kevlar/epoxy composite

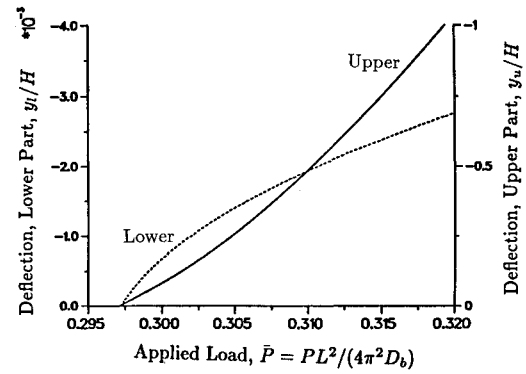

Fig. 9 Midpoint deflection of the upper (solid line) and lower (dashed line) parts from the postbuckling solution for Kevlar/epoxy with $T/H = 6$, $L/H = 200$, and delamination length $\ell/H = 60$.

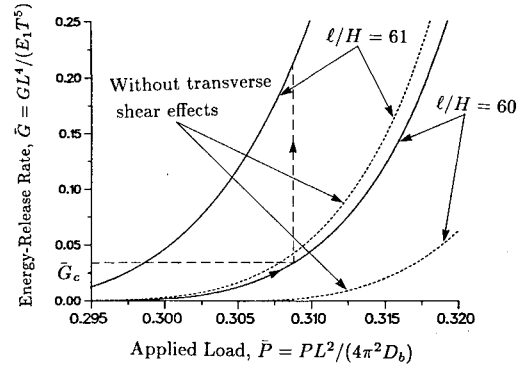

Fig. 10 Strain energy release rate vs applied compressive force during the initial postbuckling stage (Kevlar/epoxy, $T/H = 6$, $L/H = 200$).

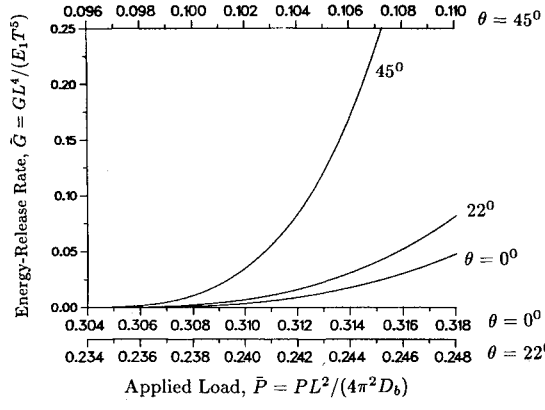

Fig. 11 Effect of lay-up angle on strain energy-release rate computations [symmetric $(\pm\theta)_s$ Kevlar/epoxy, $T/H = 6$, $L/H = 200$, $\ell/H = 60$, transverse shear effects not included]. The modulus for $\theta = 0$ deg Kevlar/epoxy has been used in normalizing the load.

beams with 0 deg, $[\pm 22\text{ deg}]_s$, and $[\pm 45\text{ deg}]_s$ angles that we performed, showed the higher lay-up angles to be more energy-absorbent than the rails with lower lay-up angles.

Finally, it should be noted that the fracture toughness may be affected by the ratio of mode I and mode II components of the energy-release rate; this cannot be captured with the J-integral method used here.

Conclusions

In summary, an analytical formulation was developed to study the compressive stability of delaminated composites. The analysis was based on a one-dimensional beam-plate

model. The perturbation method of solution that was used leads to analytical expressions for the initial postbuckling deflections. An investigation of the transverse shear effects on both the buckling load and the postbuckling behavior was also performed. These effects cause a reduction in the critical load and an increase in the energy-release rate. The phenomenological aspects of the problem were investigated over a broad range of values for the delamination size and thickness. In this study, both local buckling of the delaminated layer and mixed (combined local and global) buckling were considered as well as the possibility that global buckling may precede any other mode of instability. The postcritical characteristics such as delamination growth were studied by using the postbuckling solution to compute the energy-release rate from a J-integral formulation.

Appendix

The solution for the third order problem is given as follows. First, the nonlinear terms are included by expanding the definition for the curvature in the equation.

$$D_i \frac{\mathrm{d}}{\mathrm{d}x}\left(\frac{1}{\rho i}\right) + P_i y_i' = 0; \quad \frac{1}{\rho i} = \frac{y_i''}{\sqrt{1-(y_i')^2}} \tag{A1}$$

Therefore, the differential equation for the third order problem can be written:

$$D_i y_{i,3}''' + P_{i,0} y_{i,3}' = -P_{i,1} y_{i,2}' - P_{i,2} y_{i,1}$$

$$-D_i y_{i,1}''^2 y_{i,1}' - \frac{D_i}{2} y_{i,1}''' y_{i,1}'^2 \tag{A2}$$

As an illustrative example, the third order solution for the base plate is given by:

$$y_{b,3} = c_{b3}(1-\cos k_{b,0}x) + \mathrm{d}_{b3} x \sin k_{b,0}x$$

$$+ \frac{P_{b,1}^2}{8D_{b,0}^2 \sin k_{b,0}\ell_1} x^2 \cos k_{b,0}\ell_1 - \frac{c_{b1}^3 k_{b,0}^3}{16} \cos^3 k_{b,0}x \tag{A3}$$

$$d_{b3} = -\frac{P_{b,1}^2 (3 + 2\ell_1 k_{b,0} \cot k_{b,0}\ell_1}{8D_{b,1}^2 k_{b,0}^4 \sin k_{b,0}\ell_1} - \frac{c_{b1}^3 k_{b,0}^3}{16}$$

$$+ \frac{P_{b,2}}{2D_b k_{b,0}^2 \sin k_{b,0}\ell_1} \tag{A4}$$

The constant c_{b3} is found from condition (12). Now the equilbrium equation (4) for the third order terms is

$$M_{u,3} + M_{l,3} - M_{b,3} - M_{b,3} = P_{l,3}H/2 - P_{u,3}(T-H)/2 \tag{A5}$$

and the geometric compatibility equation (5) for the third order terms is, in turn,

$$\int_0^\ell y_{u,1}' y_{u,2}' \mathrm{d}x - \int_0^\ell y_{\ell,1}' y_{l,2}' \mathrm{d}x$$

$$= \frac{2(1-\nu_{13}\nu_{31})\ell}{wE_1 H(T-H)}\left[P_{l,3}\frac{H}{2} - P_{u,3}\frac{(T-H)}{2}\right] \tag{A6}$$

Notice that the third order moments $M_{i,3} = -D_i y_{i,3}''$ at the interface are given in terms of the already found first order and the yet undetermined second order forces. Thus, eliminating the quantity $P_{l,3}H/2 - P_{u,3}(T-H)/2$ from (A5), (A6) and taking into account that $P_{b,2} = P_{u,2} + P_{l,2}$ gives one equation for the second order forces $P_{u,2}$ and $P_{l,2}$.

The second equation needed for finding $P_{u,2}$, $P_{l,2}$ is the second order equilibrium equation (4) at the interface

$$P_{u,2}(T-H)/2 - P_{l,2}H/2 = F(P_{u,1}, P_{l,1}) \tag{A7}$$

F being the left-hand side of equation (22). The system of those two linear equations allow finding $P_{u,2}$ and $P_{l,2}$ and hence the second order applied force $P = P_{u,2} + P_{l,2}$.

References

[1]Rhodes, M.D., Williams, J.G., and Starnes, J.H. Jr., "Effect of Impact Damage on the Compression Strength of Filamentary Composite Hat-Stiffened Panels," presented at the 23rd SAMPE National Symposium and Exhibition, Anaheim, CA, May 1978; also, "Selective Application of Materials for Products and Energy," SAMPLE, Vol. 23, May 1978, pp. 300-319.

[2]Chai, H., Babcock, C.D., and Knauss, W.G., "One Dimensional Modelling of Failure in Laminated Plates by Delamination Buckling," *International Journal of Solids and Structures*, Vol. 17, No. 11, 1981, pp. 1069-1083.

[3]Simitses, G.J., Sallam, S., and Yin, W.-L., "Effect of Delamination of Axially-Loaded Homogeneous Laminated Plates," *AIAA Journal,*, Vol. 23, Sept. 1985, pp. 1437-1444.

[4]Yin, W.-L., Sallam, S.N., and Simitses, G.J., "Ultimate Axial Load Capacity of a Delaminated Beam-Plate," *AIAA Journal*, Vol. 24, Jan. 1986, pp. 123-128.

[5]Wang, S.S., Zahlan, N.M., and Suemasu, H., "Compressive Stability of Delaminated Random Short-Fiber Composites, Part I - Modeling and Methods of Analysis," *Journal of Composite Materials*, Vol. 19, 1985, pp. 296-316.

[6]Wang, S.S., Zahlan, N.M., and Suemasu, H., "Compressive Stability of Delaminated Random Short-Fiber Composites, Part II - Experimental and Analytical Results," *Journal of Composite Materials*, Vol. 19, 1985, pp. 317-333.

[7]Timoshenko, S.P. and Gere, J.M., *Theory of Elastic Stability*, McGraw-Hill, New York, 1961, pp. 1-3 and 132-135.

[8]Calcote, L.R., *The Analysis of Laminated Composite Structures*, Van Nostrand Reinhold, New York, 1969, pp. 38.

[9]Nowinski, J.L. and Ismail, I.A., "Application of a Multi-Parameter Perturbation Method to Elastostatics," *Developments in Theoretical and Applied Mechanics*, Vol. 2, 1965, pp. 35-45.

[10]Yin, W.-L. and Wang, J.T.S., "The Energy-Release Rate in the Growth of a One-Dimensional Delamination," *Journal of Applied Mechanics*, Vol. 51, 1984, pp. 939-941.

[11]Budiansky, B. and Rice, J.R., "Conservation Laws and Energy-Release Rates," *Journal of Applied Mechanics*, Vol. 40, 1973, pp. 201-203.